As for DPBF, the mechanism of photooxygenation is still a subject of controversy.[30] The reaction of DPBF with $^1O_2$ to form *o*-dibenzoylbenzene involves the apparent loss or transfer of an atom of oxygen, and thus the overall photochemical yield is expected to be two times the quantum yield of singlet oxygen. The work of Usui[23] on methylene blue sensitized photooxygenation of DPBF in methanol and tetrachloroethane supports the above prediction. However, Olmsted[18] reported that the photochemical quantum yield was almost unity, even though he carried out the experiment in a time domain similar to that of Usui. In order to interpret the present result of ΔH_r for DPBF, we must consider these mechanistic ambiguities. However, Rio and Scholl[31] suggested that the initial product is an endoperoxide which is relatively stable, while the overall reaction in methanol to form *o*-benzoylbenzene intercepted by methoxy hydroperoxide is complex. Therefore, considering the present experimental time domain, the value of ΔH_r may be ascribed to the enthalpy change to form endoperoxide.

The enthalpy change obtained here for TME in two solvents shows a considerable discrepancy (Table II). A possible interpretation for this is the solvent effect on the photooxygenation reaction of TME to form butene hydroperoxide. The reaction product hydroperoxide seems to be more stabilized in methanol than in dichloromethane owing to the formation of hydrogen bonding with methanol. However, this speculation is in conflict with the present results of ΔH_r. A satisfactory explanation for this discrepancy of ΔH_r in two solvents is not readily apparent at the present stage.

Acknowledgment. This work was partially supported by a Grant-in Aid for Scientific Research from the Ministry of Education, Science, and Culture of Japan.

(30) Wasserman, H. H.; Lipshutz, B. H. In ref 12, p 434.
(31) Rio, G.; Scholl, M. J. *J. Chem. Soc., Chem. Commun.* **1975**, 474.

New Model for the Interior of Polyelectrolyte Coatings on Electrode Surfaces. Mechanisms of Charge Transport through Protonated Poly(L-lysine) Films Containing $Fe^{III}(edta)^-$ and $Fe^{II}(edta)^{2-}$ as Counterions

Fred C. Anson,*† Jean-Michel Saveant,*‡ and Kiyotaka Shigehara†,§

Contribution No. 6677 from the Arthur Amos Noyes Laboratories, Division of Chemistry and Chemical Engineering, California Institute of Technology, Pasadena, California 91125, and Laboratoire d'Electrochimie, Universite de Paris 7, 75221 Paris, Cedex 05, France.
Received June 28, 1982

Abstract: A model is proposed for the interior of a swollen, polycationic coating equilibrated with a supporting electrolyte solution containing both electroactive and electroinactive counteranions. The coating is divided (conceptually) into two regions. The first, termed the "Donnan domains", represents the region where the counterions are confined by electrostatic forces; the second comprises the remaining volume of the coating that is assumed to be occupied by the supporting electrolyte solution. Some expected effects of this two-part structure on the electrochemical responses obtained in both steady-state and transient experiments with coated electrodes are discussed and compared with experimental results obtained with the $Fe^{III}(edta)^-/Fe^{II}(edta)^{2-}$ redox couple. The polycationic coatings employed were prepared from protonated poly(L-lysine) deposited on graphite electrodes. This particular combination of polyelectrolyte and incorporated redox couple yields rates of propagation of charge through the coating that are remarkably high in both of the regions, indicating that the open, swollen structure of the coating is particularly favorable for rapid motion of counterions. The coupling between the two propagation pathways by means of electron exchange is also quite rapid. The experimental data adhere well to the predictions of the equations derived on the basis of the two-phase model which may prove generally applicable to electrodes bearing polyelectrolyte coatings.

In the first experimental account of the exploitation of polyelectrolyte-coated electrodes to examine the kinetics of redox self-exchange reactions,[1] a simplified model, adapted from earlier work by Levich,[2] was employed to analyze steady-state data obtained with rotating disk electrodes. Subsequent theoretical analyses of the mechanisms and kinetics of charge propagation within polymer and polyelectrolyte coatings[3-6] have indicated that more intricate models may be required to account for the wide range of electrochemical responses that are obtained from electrodes coated with polymers or polyelectrolytes.[7] The kinetics of redox self-exchange processes occurring within coatings on electrodes is perhaps the simplest general case of interest, and a theoretical treatment of the kinetic behavior to be expected for the case of simple self-exchange on the basis of a more detailed model of the interior structure of polyelectrolyte coatings has been presented.[3] It proved possible to arrive at an analytical expression for the steady-state current at a coated, rotating disk electrode under all experimental conditions. In this report we present an experimental test of this new model by comparing the predictions it leads to with the observed electrochemical responses.

The essential feature of the new model employed for polyelectrolyte coatings is the existence of two phases within the coating.

† Arthur Amos Noyes Laboratories.
‡ Universite de Paris.
§ Present address: Department of Polymer Chemistry, Waseda University, 3-4-1 Ohkubo, Shinjuku-ku, Tokyo 160, Japan.

(1) Shigehara, K.; Oyama, N.; Anson, F. C. *Inorg. Chem.* **1981**, *20*, 518-522.
(2) Levich, V. G. "Physicochemical Hydrodynamics"; Prentice-Hall: Englewood Cliffs, N.J., 1962.
(3) Anson, F. C.; Saveant, J. M.; Shigehara, K. *J. Phys. Chem.* **1983**, *87*, 214.
(4) Andrieux, C. P.; Dumas-Bouchiat, J. M.; Saveant, J. M. *J. Electroanal. Chem.* **1982**, *1*, 131.
(5) Andrieux, C. P.; Saveant, J. M. *J. Electroanal. Chem.* **1982**, *134*, 163.
(6) Andrieux, C. P.; Saveant, J. M. *J. Electroanal. Chem.* **1982**, *142*, 1.
(7) Recent relevant references were cited in ref 3.

0002-7863/83/1505-1096$01.50/0

The first consists of the regions where counterions are constrained by electrostatic forces to remain in the vicinity of the fixed-charge centers in the polyelectrolyte. The second phase comprises the remaining volume of the coating that is occupied by the supporting electrolyte solution. Each of the two phases has its own modes for charge transport, and coupling between the transport processes in each phase may occur. An experimental demonstration of the existence and nature of this coupling forms an important part of this report.

Our experimental system consisted of polycationic coatings of protonated poly(L-lysine) (PLL) in which the electroactive, anionic complexes of Fe(II) and Fe(III) with edta (ethylenediaminetetraacetate) were bound by electrostatic (ion-exchange) interactions. Coatings of PLL applied to pyrolytic graphite electrodes as described in the Experimental Section are quite stable. They provide a surface coating that remains polycationic at pH values as high as 10. This attribute was exploited to examine the behavior of PLL-coated rotating disk electrodes[2] in solutions of $Fe^{III}(edta)^-$ at pH values high enough to assure the stability of both $Fe^{II}(edta)^{2-}$ and $Fe^{III}(edta)^-$.

Protonated PLL coatings undergo very extensive swelling in aqueous electrolytes to produce films with relatively large separations between the polymer chains. This feature accentuates the role of the reactants that are dissolved in the solution occupying the empty spaces within the swollen coatings and proved useful in testing the predictions of the two-phase kinetic model. The results obtained strongly support this model and provide considerable insight into the nature of redox equilibria and ionic motions within polyelectrolyte coatings on electrodes.

Experimental Section

Materials. Poly(L-lysine) hydrobromide (PLL) was prepared by the conventional ring-opening polymerization of *N*-carbobenzoxy-L-lysine initiated by ethylamine in dry, deaerated dimethylformamide.[8] Following the polymerization the carbobenzoxy group was removed by hydrolysis with 20% HBr in acetic acid to yield PLL.

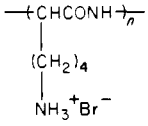

The degree of polymerization, n, was estimated as 2×10^3 from vapor-pressure osmometry of solutions of the poly(*N*-carbobenzoxy-L-lysine) precursor prior to its hydrolysis.[9]

Sodium ethylenediaminetetraacetatoferrate(III), NaFe(edta),[10] disodium ethylenediaminetetraacetatozincate(II), $Na_2Zn(edta)$,[10] and ammonium dioxalatodiamminecobaltate(III), $NH_4[Co(C_2O_4)_2(NH_3)_2]$[11] were prepared and purified according to the procedures cited. Solutions of $Fe^{II}(edta)^{2-}$ and $Fe^{III}(heedta)$ (β-hydroxyethylethylenediaminetriacetatoiron(III)) were prepared by mixing equivalent amounts of the ligands with $FeSO_4$ or $Fe(NO_3)_3$ in buffered, deaerated supporting electrolyte solutions. Other chemicals were reagent grade and were used without further purification. Laboratory distilled water was further treated by passage through a purification train (Barnsted Nanopure). Solutions were deaerated by bubbling with prepurified argon. Pyrolytic graphite electrodes (Union Carbide Co., Chicago, Ill.) with basal planes exposed were cut and mounted as previously described.[12]

Apparatus and Procedures. Cyclic and rotating disk voltammetry were conducted with apparatus and by procedures that have been described.[1,12] Chronocoulometric measurements were carried out with a computer-controlled electrochemical apparatus similar to that described previously.[13] For the reduction of $Fe^{III}(edta)^-$ the potential was stepped from +0.3 to −0.4 V, and these potentials were reversed for measurements in the oxidation of $Fe^{II}(edta)^{2-}$. The latter experiments were actually conducted with solutions of $Fe^{III}(edta)^-$ in which $Fe^{II}(edta)^{2-}$ was generated electrolytically at the electrode surface by holding its potential at −0.4 V for 60 s just before the potential was stepped to +0.3 V.

Adherent coatings of PLL were produced by transferring an aliquot of an 0.5 wt.% aqueous solution of the polymer to the surface of a freshly cleaved graphite electrode. The solvent was allowed to evaporate at room temperature (ca. 20 min). The resulting, slightly moist film was then heated with a heat gun to ca. 80 °C for 30 s. This final step produced much more stable films thought to contain chains that are partially cross-linked by hydrogen bonding. In solutions of PLL the configuration of the polyelectrolyte changes from a random coil to an α helix at ca. pH 10.[14,15] Upon heating, an insoluble material separates with a β-sheet structure.[15] This material remains quite insoluble at all pH values and electrolyte compositions, and we believe that the coatings of PLL may assume the β-sheet structure when they are heated to 80 °C during their preparation.

Better PLL coatings resulted when the aqueous polyelectrolyte solution from which the films were prepared were several months old. It is possible that some of the structural changes required for the transformation from random coils to β-sheets occur slowly but spontaneously in the solution.

Estimates of the thickness of wet, swollen films of PLL were obtained by the following procedure. A thin (~1 mm) cylindrical pyrolytic graphite electrode was hand-polished on both top and bottom faces with moist silicon carbide. A PLL coating was then applied to one of the polished faces by the procedure described above. The coating was equilibrated with each solution of interest until all swelling appeared to be complete. The electrode was then removed from the solution and the droplet of solution adhering to the coating was carefully removed by the wicking action of a small piece of filter paper. The coated electrode's dimension was then measured carefully with a micrometer while observing the interface between the coating and the micrometer head under a magnifying glass to avoid crushing the coating. The difference in this micrometer reading and that obtained with the original uncoated electrode was taken to be the thickness of the swollen film. This procedure proved reliable with films having thicknesses of several hundred microns or more.

The quantities of $Fe^{II}(edta)^{2-}$ incorporated by PLL coatings were determined by coulometric assays of electrodes that were equilibrated with solutions of $Fe^{II}(edta)^{2-}$ and then transferred in a glovebag under an argon atmosphere to pure supporting electrolyte where the electrode potential was stepped from −0.4 to +0.3 V to oxidize the incorporated complex to $Fe^{III}(edta)^-$. The resulting anodic current was integrated until it fell to background levels (~10 s). The transfer and current integration were carried out as rapidly as possible, but some small loss of $Fe^{II}(edta)^{2-}$ from the coating was unavoidable because it gradually departs from PLL coatings in pure supporting electrolyte solutions. To correct for these losses a series of electrode transfer experiments was conducted with successively greater elapsed times between the transfer and the coulometric assays. The resulting, slowly decreasing values of $\Gamma_{Fe(II)}$ were extrapolated to zero time to obtain the quantity of complex in the film equilibrated with each solution of $Fe^{II}(edta)^{2-}$.

Estimates of the quantities of $Fe^{III}(edta)^-$ and $Fe^{III}(heedta)$ incorporated by PLL films were obtained spectrophotometrically by applying PLL coatings to optically transparent plates of poly(ethylenephthalate) and equilibrating the coatings with solutions containing the ion of interest. The plates were then removed and shaken lightly to remove any adhering droplets of the solution, and the absorbance of the coatings at 330 nm was compared with that of standard solutions of the ions by means of a Hewlett-Packard Model 8450A spectrophotometer.

Experiments were conducted at the laboratory temperature, 22 ± 2 °C. Potentials were measured and are reported with respect to a sodium chloride saturated calomel electrode, SSCE.

Results and Discussion

Description of the Model. Figure 1 gives a schematic picture of the situation we envisage inside a swollen polycationic coating such as polylysine in which the electroactive anions Z^- and Z^{2-} are incorporated along with the ionic components of the supporting electrolyte, C^+ and X^-. The swollen coating contains two domains. The tangled, polyelectrolyte chains with their accompanying counterions are separated by empty regions that are filled up by the supporting electrolyte solution with which the coating is equilibrated. Donnan equilibria[16] are assumed to prevail within

(8) Doty, P. *J. Am. Chem. Soc.* **1957**, *79*, 396. Iwakura, Y.; Uno, K.; Oya, M. *J. Polym. Sci Part A* **1967**, *6*, 2867. Oya, M.; Takahashi, T.; Katakai, R. *J. Polym. Sci., Polym. Chem. Ed.* **1976**, *14*, 2065.
(9) Wachter, A. H.; Simon, W. *Anal. Chem.* **1969**, *41*, 90.
(10) Sawyer, D. T.; McKinnie, J. M. *J. Am. Chem. Soc.* **1960**, *82*, 4191.
(11) Risenfeld, E. H.; Klementi, R. *Z. Anorg. Chem.* **1922**, *124*, 1.
(12) Oyama, N.; Anson, F. C. *Anal. Chem.* **1980**, *52*, 1192–1198.
(13) Lauer, G.; Abel, R.; Anson, F. C. *Anal. Chem.* **1967**, *39*, 765–769.
(14) Padden, F. J., Jr.; Keith, H. D.; Giannoni, G. *Biopolymers* **1969**, *7*, 793.
(15) Sameli, U.; Taub, W. *J. Mol. Biol.* **1965**, *12*, 205, and references therein.
(16) Bard, A. J.; Faulkner, L. R. "Electrochemical Methods"; Wiley: New York, 1980; p 76.

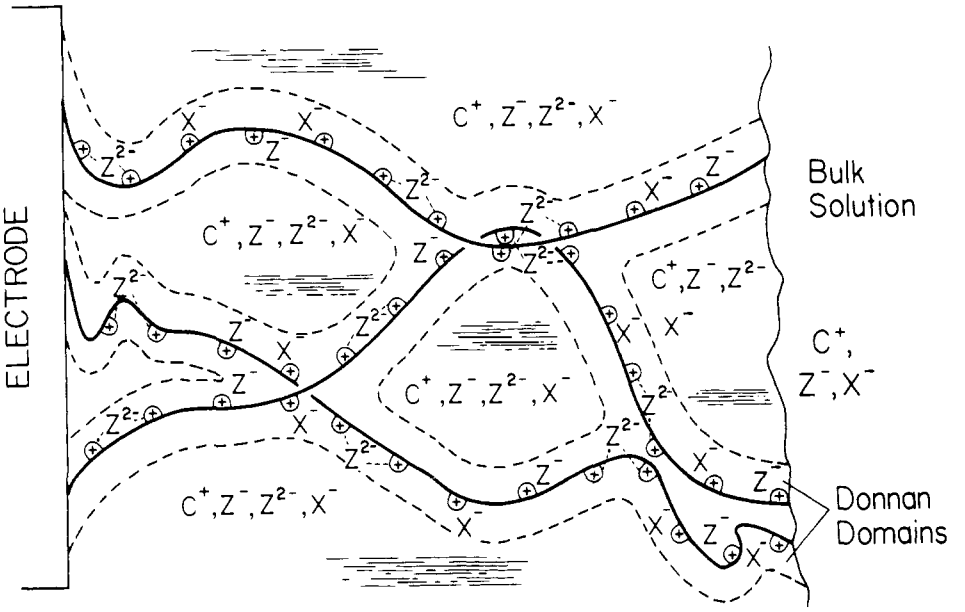

Figure 1. Schematic model for a portion of a swollen polycationic film on an electrode surface. The film has been equilibrated with a solution containing an electroinactive supporting electrolyte composed of C^+X^- and the oxidized half of an electroactive couple, Z^-/Z^{2-}. The electrode potential is adjusted to the limiting current plateau for the reduction of Z^- to Z^{2-}. Solid lines represent the polyelectrolyte chains. The dashed lines indicate the regions of extension of the "Donnan domains" containing the electrostatic fields generated by the fixed cationic sites on the chains. The remaining, empty space is filled by the supporting electrolyte solution that permeates the coating.

the volumes close to the polyelectrolyte chains (indicated by the dashed lines) to exclude cationic co-ions and attract anionic counterions. The solution that occupies the regions outside of the "Donnan domains" will have a composition that is determined by the composition of the bulk supporting electrolyte solution. With highly swollen polymeric coatings the composition of the electrolyte solution inside and outside the coating may be essentially identical, but, in general, some partitioning of various components of the electrolyte may occur. Partition coefficients, κ, are used to express the ratio of the concentrations of species of interest in the solution phase inside the coating and in the bulk supporting electrolyte solution.[3]

The presence of two phases within the polyelectrolyte coating requires that two types of exchange reactions be considered between pairs of oxidized and reduced reactant within the coating: in-phase exchange and cross-phase exchange. In-phase exchange involves reactions in which both members of the exchanging pair (e.g., Z^- and Z^{2-} in Figure 1) are present in the same phase. Cross-phase exchange involves oxidized and reduced reactants that begin in two different phases and end up in the opposite phase as a result of the exchange reaction. Cross-phase exchange may proceed either by the physical motion of the two reactants, i.e., cross-phase place exchange, or by electron transfer between the two reactants that remain in their respective phases, i.e., cross-phase electron exchange.

When the electrode potential is adjusted to a value where Z^- at the coating-electrode interface is rapidly reduced to Z^{2-}, the magnitude of the resulting current is governed by the rate at which charge can be carried across the coating. The charge is propagated through the solution phase within the coating by diffusion of the reactants. Such diffusion could, in principle, involve both the usual physical motion of the reactants as well as electron exchange between reactant pairs. However, the latter is known to be negligible except with very high concentrations of redox couples.[17]

Charge can also be propagated through the Donnan domains by both physical displacement of the ions without change in oxidation level or by electron exchange between pairs of reactant ions without their physical displacement. The latter process must be considered a priori because the high concentration of fixed charge sites inside the Donnan domains can produce very high reactant concentrations. Charge propagation by electron exchange has been shown to appear diffusion-like and the relationship between the rate of electron exchange and the effective diffusion coefficient has been established.[18] Physical displacement of the ions might involve nothing more than a solution-like diffusion process proceeding in the Donnan domains. However, another possible mechanism might be termed *ion hopping* between adjacent sites. As for electron hopping (i.e., electron exchange), ion hopping would appear diffusion-like and the relationship between the rate constant for ion hopping and the diffusion coefficient would be the same.[18] It follows that, whatever its exact mechanism, a single effective diffusion coefficient can be applied to charge propagation within the Donnan domains.

Thus, there are two parallel pathways for charge propagation through the polyelectrolyte coating, one within and the other outside of the Donnan domains. The two pathways are coupled by the cross-phase electron- and place-exchange reactions whose rates determine the extent of the coupling. The current obtained on the plateau of current–potential curves recorded with coated, rotating disk electrodes will depend upon the interplay of the three processes just described.

Charge Propagation in the Two-Phase Coating. The contributions of the three processes for charge propagation can be expressed in terms of three "characteristic current densities", i_S, i_E, and i_k.[3,5]

The first, i_S, measures the rate of diffusion within the coating of the reactant that is located outside of the Donnan domains. Its magnitude is given by

$$i_S = FD_S\kappa C_A^0/\Phi \quad (1)$$

where F is the faraday, D_S is the diffusion coefficient of the reactant in the regions of the coating outside of the Donnan domains, κ is the partition coefficient that gives the equilibrium ratio of the concentration of the reactant in the bulk solution to that in the solution phase within the coating, C_A^0 is the reactant concentration in the bulk of the solution, and Φ is the thickness of the coating.

In ref 3 and in what follows, A and B designate the oxidized and reduced forms of the reactant in the solution phase within the coating and P and Q designate the same species when present in the Donnan domains. Thus, A and P correspond to Z^- (e.g., $Fe^{III}(edta)^-$) and B and Q correspond to Z^{2-} (e.g., $Fe^{II}(edta)^{2-}$) in Figure 1.

(17) Dahms, H. *J. Phys. Chem.* **1968**, *72*, 362.

(18) Andrieux, C. P.; Saveant, J. M. *J. Electroanal. Chem.* **1980**, *111*, 377. Laviron, E. *Ibid.* **1980**, *112*, 1.

The second characteristic current density, i_E, measures the rate at which charge is transported within the Donnan domains. The magnitude of i_E is given by

$$i_E = \frac{FD_E C_p^0}{\Phi} = \frac{FD_E \Gamma_p^0}{\Phi^2} \quad (2)$$

where D_E is the apparent diffusion coefficient governing the diffusion-like transport of the reactant and C_p^0 and Γ_p^0 are the concentration and the total quantity of reactant, respectively, within the Donnan domains.[19]

The third characteristic current density, i_k, measures the sum of the electron-exchange and place-exchange rates between the reactant and coreactant inside and outside the Donnan domains. The magnitude of i_k is given by

$$i_k = k_{ap} F \Gamma_p^0 \quad (3)$$

where k_{ap} is the apparent rate constant governing the overall cross-phase exchange reaction. k_{ap} represents a composite rate constant whose value depends upon the rates of the cross-phase electron- and place-exchange reactions. In addition, k_{ap} can be affected by the rates of cross-phase interchange reactions between each of the two electroactive complexes and the counterions of the fixed charge groups of the PLL (reactions 4 and 5) even though no electron transfer between phases is involved.[3]

$$A \underset{k_2}{\overset{k_1}{\rightleftharpoons}} P \quad (4)$$

$$B \underset{k_2}{\overset{k_1}{\rightleftharpoons}} Q \quad (5)$$

The composite nature of k_{ap} is exposed in the equation

$$k_{ap} = (k\kappa C_A^0 + k_2) \quad (6)$$

where k is the rate constant governing the sum of the cross-phase electron- and place-exchange reactions and k_2 is the constant governing the backward rate of cross-phase interchange.[3] The kinetics of reactions 4 and 5 are expected to be pseudo-first-order so long as the concentrations of counterions within the Donnan domains and surrounding solution (X^- in Figure 1) are large compared with those of the reactants. (For the Donnan domains this implies that the quantity of incorporated reactant be small enough so that the "incorporation isotherm" is linear.)

The sum of the cross-phase electron- and place-exchange reactions is represented by

$$A + Q \underset{k}{\overset{k}{\rightleftharpoons}} B + P \quad (7)$$

which will exhibit second-order kinetics. The rate constant, k, is shown as equal for both directions of reaction 7 because it is regarded as a true self-exchange reaction. The formal potential of the $Fe^{III}(edta)^-/Fe^{II}(edta)^{2-}$ couple incorporated in PLL coatings is nearly the same as the formal potential of the couple in solution (Figure 2) so that it is reasonable to regard the equilibrium constant for reaction 7 to be close to unity.

When the rate of cross-phase place-exchange between the coreactants is low compared with their rate of cross-phase electron exchange, k can be identified with the latter process. Otherwise, k represents a composite rate constant with a value that depends on the rates of both modes of cross-phase exchange.[3]

Experimental Tests of the Models. Cyclic Voltammetry. Figure 2 compares the cyclic voltammograms for a solution of $Fe^{III}(edta)^-$ at a bare graphite electrode (curve A) with that for $Fe^{III}(edta)^-$ incorporated in a PLL coating and transferred to pure supporting electrolyte (curve B). The average of the cathodic and anodic peak potentials of the two voltammograms are almost the same, 0.13 vs. 0.12 V for voltammograms A and B, respectively. The formal potential of redox couples measured in solution and when incorporated in polyelectrolyte coatings will be different unless the equilibrium binding constants of the oxidized and reduced forms of the redox couple with the polyelectrolyte are equal. The near equivalence of the formal potentials of the $Fe^{III/II}$–edta couples shown in Figure 2 indicates that the equilibrium binding constants for the two oxidation states differ by only a small factor despite the higher charge carried by the $Fe(edta)^{2-}$ complex. This somewhat surprising equivalence could result from the relatively large size and low charge density of the complex ions. In any case, the near equivalence of the two formal potentials made the $Fe^{III}(edta)^-/Fe^{II}(edta)^{2-}$ couple a good system for experimental studies of a true self-exchange reaction occurring within a polyelectrolyte coating.

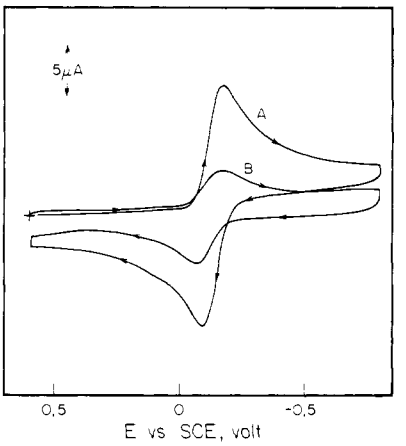

Figure 2. Cyclic voltammograms for $Fe^{III}(edta)^-$: (A) 0.5 mM $Fe^{III}(edta)^-$ at a bare graphite electrode; (B) after the electrode was coated with 2.6×10^{-7} mol cm^{-2} of PLL, soaked in a 0.5 mM $Fe^{III}(edta)^-$ solution, and transferred to pure supporting electrolyte. Some loss of the $Fe^{III}(edta)^-$ occurred during the transfer. Scan rate was 100 mV s^{-1} for both curves; supporting electrolyte, 0.2 M CH_3COONa at pH 5.5.

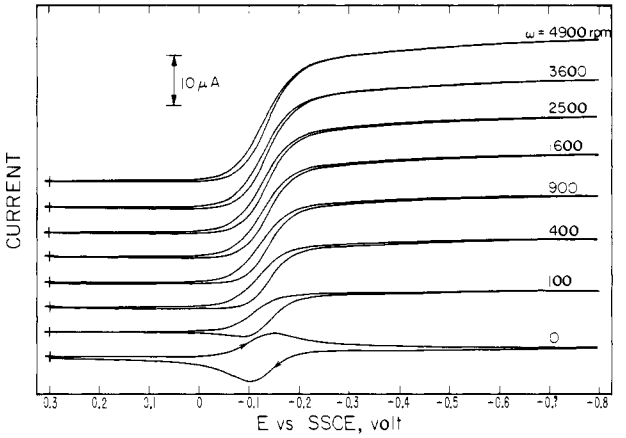

Figure 3. Current–potential curves for the reduction of 0.55 mM $Fe^{III}(edta)^-$ at a rotating graphite disk electrode coated with 2.6×10^{-7} mol cm^{-2} of PLL. Supporting electrolyte, 0.2 M CH_3COONa at pH 5; potential scan rate, 5 mV s^{-1}; electrode area, 0.189 cm^2.

Limiting Currents at Rotating Disk Electrodes Coated with PLL. Pyrolytic graphite electrodes coated with PLL and mounted in rotating disk configurations were used to record current–potential curves for solutions of $Fe^{III}(edta)^-$. Some representative curves are shown in Figure 3. The steady-state current on the plateau of each wave corresponds to the reduction of $Fe^{III}(edta)^-$ to $Fe^{II}(edta)^{2-}$. Sets of curves were recorded for electrodes with increasingly thick coatings of PLL, and the resulting Levich plots[2]

(19) Equations 1 and 2 and, more generally, the whole treatment on which the data analysis is based[3] involve the approximation that the properties of the polymer film are uniform in the direction perpendicular to the electrode surface. This approximation allows the use of conventional concentrations of the reactants obtained by averaging the actual concentrations over the whole area of a section of the film parallel to the electrode surface. Thus, C_p^0 is defined as Γ_p^0/Φ. The actual concentration of the incorporated reactant in the Donnan domains C_p^* (which is larger than C_p^0) could be written as $C_p^* = \Gamma_p^0/\Phi\gamma$, where γ is the fraction of the total volume of the film occupied by the Donnan domains.

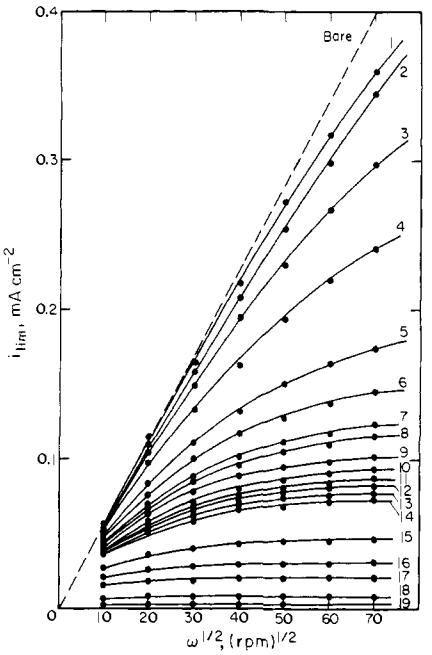

Figure 4. Levich plots for the reduction of 0.55 mM $Fe^{III}(edta)^-$ at rotating graphite disks coated with PLL. The quantities of PLL in the coatings for curves 1 to 19 are given in Table I. The dashed line is the response obtained at a bare electrode; other conditions as in Figure 3.

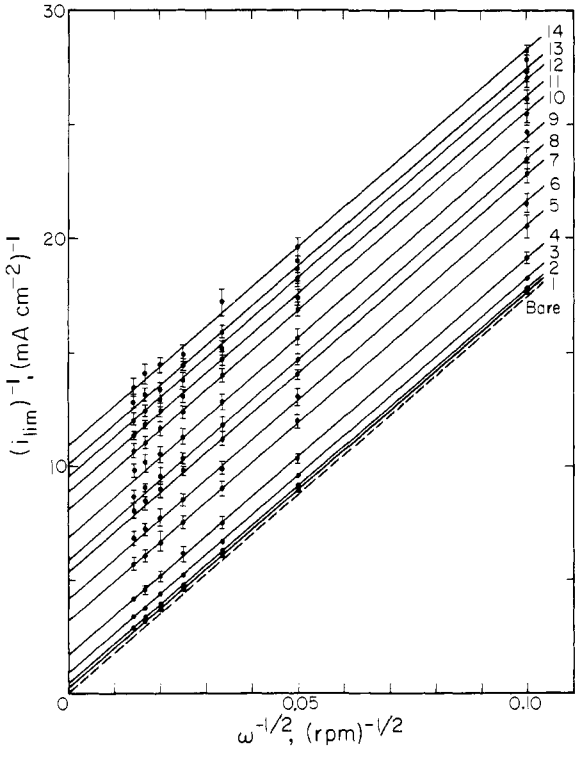

Figure 5. Koutecky–Levich plots of the data from curves 1 to 14 of Figure 4.

of the limiting current vs. the square root of the electrode rotation rate (i_{lim} vs. $\omega^{1/2}$) are shown in Figure 4. The increasing deviations of the points from the linear response obtained at the bare graphite electrode before it was coated with PLL reflect the increasing mismatch between the flux of electrons traversing the PLL coating and the flux of $Fe^{III}(edta)^-$ ions that are propelled to the PLL-electrolyte interface by the rotation of the electrode. To compare the observed behavior with that predicted on the basis of the kinetic model it is convenient[3] to prepare Koutecky–Levich plots[12,20] of

(20) Koutecky, J.; Levich, V. G. *Zh. Fiz. Khim.* **1956**, *32*, 1565.

Table I. Film Current Densities, i_F, Evaluated from Intercepts of Koutecky–Levich Plots for the Reduction of $Fe^{III}(edta)^-$ at PLL-Coated Graphite Electrodes[a]

expt no.	$10^7\Gamma_{PLL}$, mol cm^{-2}	$10^3\Phi$,[b] cm	$10^{10}\Gamma_{Fe(II)}$,[c] mol cm^{-2}	$10^2 i_F$,[e] mA cm^{-2}
1	0.041	0.0261	0.61	425
2	0.081	0.052	1.19	214
3	0.161	0.10	2.35	109
4	0.32	0.20	4.69	58.8
5	0.64	0.41	8.42	31.3
6	0.96	0.61	12.6	24.0
7	1.28	0.82	16.8	18.7
8	1.93	1.23	24.9	17.3
9	2.57	1.64	33.3	14.6
10	3.85	2.45	49.5	12.3
11	5.13	3.27	65.7	11.3
12	7.70	4.90	98.6	10.5
	7.70	4.90	104[d]	10.5
13	10.3	6.56	129	9.9
	10.3	6.56	132[d]	9.9
14	12.8	8.15	161	9.2
	12.8	8.15	176[d]	9.2
15	27.9	17.8	385[d]	5.37
16	55.8	35.5	731[d]	3.39
17	112	71.3	1540[d]	2.25
18	224	143	3101[d]	0.90
19	631	398	8630[d]	0.34

[a] The test solution consisted of 0.55 mM $Fe^{III}(edta)^-$ in a supporting electrolyte of 0.2 M CH_3COONa at pH 5.5. [b] Measured with a micrometer for the thicker coatings and assumed to vary linearly with PLL (see Experimental Section). [c] Total quantity of $Fe^{II}(edta)^{2-}$ present in the Donnan domains. [d] Measured spectrophotometrically with coating of same thickness deposited on transparent poly(ethylenephthalate) plate. [e] From the intercepts of plots such as those in Figure 5.

$(i_{lim})^{-1}$ vs. $\omega^{-1/2}$. Figure 5 redisplays much of the data of Figure 4 in the Koutecky–Levich format. The linearity of the plots with slopes that match the slope at a bare electrode shows that the limiting currents obey the Koutecky–Levich equation[20]

$$\frac{1}{i_{lim}} = \frac{1}{i_A} + \frac{1}{i_F} \tag{8}$$

where i_A is the rotation rate-dependent Levich current[3] and i_F is the film current that is independent of rotation rate.[21]

Properties of the Film Current. In ref 3 the following general expression for the film current was derived in terms of the three characteristic currents defined by eq 1, 2, and 3:

$$\frac{1}{i_F} = \frac{1}{i_S + i_E}\left[1 + \frac{i_E}{i_S}\frac{\tanh\left(\frac{i_k}{i_S} + \frac{i_k}{i_E}\right)^{1/2}}{\left(\frac{i_k}{i_S} + \frac{i_k}{i_E}\right)^{1/2}}\right] \tag{9}$$

Equation 9 takes simpler, limiting forms with sufficiently thin or thick films.[3] With sufficiently thin films, i_k becomes much smaller than both i_S and i_E, and the second term inside the brackets in eq 9 reduces to i_E/i_S so that $1/i_F = 1/i_S$. With sufficiently thick films, i_k becomes much greater than both i_S and i_E and eq 9 reduces to $1/i_F = 1/(i_S + i_E)$. We attempted to observe these limiting cases of eq 9 by evaluating values of i_F for a wide range of film thicknesses. The resulting values of i_F, obtained from the intercepts of the Koutecky–Levich plots in Figure 5, are summarized in Table I. A log–log plot of i_F vs. the film thickness, Φ, is shown in Figure 6.

For the thinnest films the experimental values of i_F do lie on a straight line from which the value of i_S for each film thickness can be read. A linear asymptote is also evident with the thickest films from which $(i_S + i_E)$ can be read for each film thickness. Thus, the two limiting asymptotes in Figure 6 provide values for

(21) In eq 8 and those following it, the symbolism corresponds to that employed in ref 3 but differs somewhat from that in ref 1 and 12.

Table II. Concentration Dependences of the Film Current Density and of the Apparent Self-Exchange Constant

$[Fe^{III}(edta)^-]$,[a] mM	$10^3\Phi$,[b] cm	$10^9\Gamma_{Fe(II)}$,[c] mol cm^{-2}	i_E,[d] mA cm^{-2}	i_F,[e] mA cm^{-2}	i_S,[f] mA cm^{-2}	i_k,[g] mA cm^{-2}	k_{ap},[h] s^{-1}
0.55	1.23	2.49	1.06	0.17	0.092	0.031	1.28
0.94	1.16	4.31	2.07	0.29	0.15	0.053	1.33
1.87	1.05	8.52	5.00	0.89	0.34	2.70	3.29
3.74	0.90	17.0	13.6	2.72	0.75	12.9	7.8
7.48	0.69	33.9	46.0	7.82	1.88	40.9	12.5

[a] Supporting electrolyte: 0.2 M CH_3COONa at pH 5.5. [b] The electrode was coated with 1.9×10^{-7} mol cm^{-2} of PLL. The thickness of the coating was calculated from micrometric measurements on thicker films that were equilibrated with the same solutions. [c] Total quantity of $Fe^{II}(edta)^{2-}$ present in the Donnan domains. [d] Calculated from equation 3 using $D_E = 6.7 \times 10^{-6}$ cm^2 s^{-1} (see text). [e] Evaluated from the intercepts of Koutecky-Levich plots. [f] Measured from the intercepts of Koutecky-Levich plots of rotating disk data obtained with solutions of the surrogate reactant, $[Co(C_2O_4)_2(NH_3)_2]^-$ (see text). [g] Calculated from equation 9. [h] Calculated from equation 3.

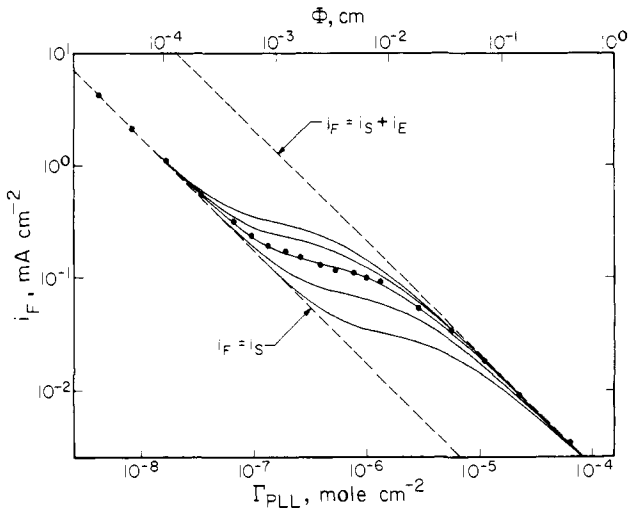

Figure 6. Comparison of experimental film currents (●) with those calculated from eq 9. The solid curves were calculated from eq 9 using the value of i_k obtained from eq 3 and values of i_S and i_E obtained from the two linear asymptotes (dashed lines) (see text). From top to bottom, the solid curves correspond to k_{ap} = 6.5, 3.25, 1.3, 0.325, and 0.065 s^{-1}.

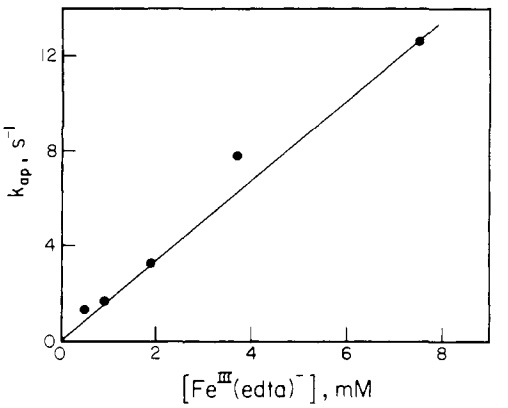

Figure 7. Variation of the apparent first-order rate constant for cross-phase exchange with the bulk concentration of $Fe^{III}(edta)^-$.

both i_S and i_E at any film thickness directly from the rotating disk data.

Evaluation of D_S and D_E. The values of i_S and i_E obtained from Figure 6 may be employed with eq 1 and 2 to calculate values of the two diffusion coefficients, D_S and D_E. The values obtained are $D_S = 2.1 \times 10^{-6}$ cm^2 s^{-1} and $D_E = 6.7 \times 10^{-6}$ cm^2 s^{-1}. We will defer comments on the magnitudes of these two constants to a later section.

Evaluation of k. Values of i_S and i_E, obtained by extrapolation of the linear asymptotes in Figure 6 to intermediate film thicknesses, were employed with eq 3 and 9 to calculate values of i_F for various values of k_{ap}. The results are shown by the solid curves in Figure 6. The calculated curve with the best fit to the experimental points was obtained for k_{ap} = 1.3 s^{-1}. The good adherence of the experimental data to the curve calculated for this value of k_{ap} over the entire range of coating thicknesses provides strong support for the two-phase kinetic model that was used to derive eq 9.[3]

To obtain k from the measured value of k_{ap} it is necessary to estimate separately the contributions to the overall exchange process of cross-phase interchange (reactions 4 and 5) and of the sum of cross-phase electron and place exchange (reaction 7). A measurement of the dependence of i_k on C_A^0 (i.e., on the concentration of $Fe^{III}(edta)^-$) was required to assess the magnitudes of these two contributions. Accordingly, film currents were evaluated for several concentrations of $Fe^{III}(edta)^-$ from measurements with a rotating disk electrode coated with a fixed amount of PLL. The corresponding values of i_k were calculated at each concentration by means of eq 9. To do so, values of i_E and i_S were also required. i_E was calculated from eq 2 using the value of D_E (6.7×10^{-6} cm^2 s^{-1}) obtained previously from Figure 6. (D_E shows no significant dependence on C_A^0 (Table V)). The required value of i_S could not be calculated from eq 3 using the value of D_S resulting from the thin-film asymptote in Figure 6 because D_S is not independent of C_A^0 (Figure 9). Therefore, i_S was determined for each concentration of reactant from the intercepts of Koutecky–Levich plots of rotating disk limiting currents. The actual reactant of interest, $Fe^{III}(edta)^-$, could not be employed in these experiments because the film currents would then contain contributions from both i_S and i_E. To eliminate the contributions from i_E, the rotating disk experiments were conducted with solutions of a surrogate reactant, $[Co(C_2O_4)_2(NH_3)_2]^-$, having the same uninegative charge as $Fe^{III}(edta)^-$ but with totally different chemical properties that precluded the occurrence of electron exchange between oxidized and reduced forms of the reactant. Upon reduction, $[Co(C_2O_4)_2(NH_3)_2]^-$ rapidly decomposes into products (Co^{II}, $C_2O_4^{2-}$, NH_4^+) that are both electroinactive at the potentials of interest and that do not react with the initial complex. In addition to the surrogate reactant the test solutions also contained an equal concentration of the electroinactive $Zn^{II}(edta)^{2-}$ complex which served two functions: the complex binds to the PLL chains where it was assumed to produce the same degree of electrostatic cross-linking[1] as does $Fe(edta)^{2-}$ at the same concentration; the dinegative $Zn(edta)^{2-}$ complex also binds preferentially to the PLL chains so that the rate and magnitude of the binding of $[Co(C_2O_4)_2(NH_3)_2]^-$ by the Donnan domains were too small to contribute to the measured film currents. The reliability of this surrogate reactant procedure was verified by noting that the value of i_S obtained with the 0.55 mM solution of the surrogate reactant (0.092 mA cm^{-2}) agreed with that read directly from the thin film limiting asymptote in Figure 6 for the same film thickness and concentration of $Fe^{III}(edta)^-$ (0.091 mA cm^{-2}). The values of i_k resulting from the two sets of experiments just described were converted to the corresponding values of k_{ap} (eq 3) that are summarized in Table II. A plot of k_{ap} as a function of the bulk concentration of $Fe^{III}(edta)^-$ is shown in Figure 7. A fair approximation to the linear plot expected on the basis of eq 6 is observed. This provides additional evidence that the kinetic model that led to eq 6 gives a reasonable portrayal of the phenomena occurring within these polyelectrolyte coatings.

The slope of the line in Figure 7 corresponds to $\kappa k = 2 \times 10^3$ M^{-1} s^{-1}. To evaluate k itself, κ was estimated by means of the

Table III. Spectrophotometric Evaluations of κ for the Incorporation of $Fe^{III}(edta)^-$ and $Fe^{III}(heedta)$ in PLL Coatings

$[Fe^{III}(edta)^-]$,[a] mM	Φ,[b] cm	abs[c]	concn of complex in PLL coating,[d] mM	κ
0.55	0.028	0.0438	0.56	1.02
0.94	0.033	0.0794	0.86	0.91
1.87	0.021	0.093	1.58	0.84
3.74	0.016	0.173	3.86	1.03
7.48	0.019	0.380	7.14	0.95
$[Fe^{III}(heedta)]$,[a] mM				
0.55	0.034	0.053	0.53	0.96
1.87	0.028	0.15	1.82	0.97
7.48	0.036	0.78	7.36	0.98

[a] The loading solution (pH 5.5) also contained 0.2 M CH_3COONa and $Zn^{II}(edta)^{2-}$ at the same concentration as the Fe(III) complex. [b] Coating thickness calculated from the quantity of PLL in each coating and the density of swollen coatings on graphite disks measured as described in the Experimental Section. [c] Measured absorbance of the coating at 330 nm. [d] Calculated from the absorbance, coating thickness, and molar absorbances, ϵ, of the incorporated complex: for $Fe^{III}(edta)^-$, $\epsilon_{330} = 2.8 \times 10^3$ L mol^{-1} cm^{-1}, for $Fe^{III}(heedta)$, $\epsilon_{330} = 2.95 \times 10^3$ L mol^{-1} cm^{-1}.

spectrophotometric procedure described in the Experimental Section. The value of κ desired is that corresponding to the entry of $Fe^{III}(edta)^-$ into PLL coatings in which significant quantities of $Fe^{II}(edta)^{2-}$ are electrostatically held within the Donnan domains. To provide a similar coating structure during the spectrophotometric measurements, equal concentrations of $Zn(edta)^{2-}$ were added to the $Fe^{III}(edta)^-$ solutions. The spectrophotometric data and corresponding values of κ are summarized in Table III. The data show that the amount of $Fe^{III}(edta)^-$ present in the PLL coatings is no larger than expected from its bulk concentration in the solutions and the volume of the coating. The presence of the more highly charged $Zn(edta)^{2-}$ anion apparently prevents the incorporation of significant quantities of $Fe^{III}(edta)^-$ by the Donnan domains. This surmise was confirmed by also measuring the quantities of the uncharged $Fe^{III}(heedta)$ complex that was incorporated by the same PLL coatings (Table III). The ratio of the concentration of the complex in the bulk solution to that in the solution phase within the coating is essentially unity, confirming that there was no significant partitioning of either complex between the solution phases inside and outside the coatings. On the basis of the data in Table III κ was set equal to unity.

Since $\kappa = 1$, the slope of the line in Figure 7 corresponds to $k = 2 \times 10^3$ M^{-1} s^{-1}. The intercept of the line, representing the value of k_2, falls too close to the origin to be measured reliably. However, this small value of k_2 indicates that cross-phase interchange (reactions 4 and 5) is too slow to affect the plateau currents at the rotating disk electrode (note that the interchange reactions become relatively less and less important as C_A^0 increases). It therefore seems likely that the component of reaction 7 that arises from cross-phase place exchange will also make a negligible contribution to the overall self-exchange process. Thus, the evidence points to cross-phase electron exchange between $Fe^{II}(edta)^{2-}$ inside the Donnan domains and $Fe^{III}(edta)^-$ in the solution phase as the dominant self-exchange pathway in these PLL coatings.

No experimental measurement of k for the analogous electron self-exchange reaction between $Fe^{II}(edta)^{2-}$-$Fe^{III}(edta)^-$ in homogeneous solution has been reported, but it has been assumed to be approximately equal to the rate constant for the cross-reaction between $Fe^{II}(edta)^{2-}$ and the closely related $Fe^{III}(cydta)$ complex (cydta = *trans*-1,2-diaminocyclohexanetetraacetate) which has been measured.[22] This cross-reaction rate constant

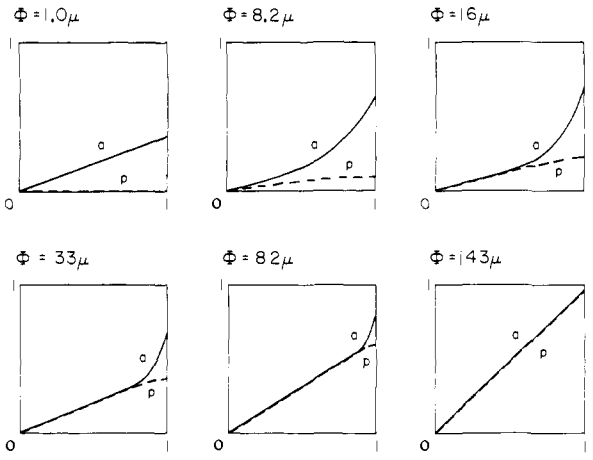

Figure 8. Calculated dimensionless concentration profiles of $Fe^{III}(edta)^-$ within some of the coatings of Table I. The ordinate is the ratio of the concentration of $Fe^{III}(edta)^-$ to its equilibrium concentration in the absence of current flow. The solid and dashed lines give this concentration ratio outside (a) and inside (p) the Donnan domains, respectively. The abscissa is the dimensionless distance X/Φ from the electrode/coating interface. Φ is the coating thickness. The curves correspond to an electrode rotation rate of 1907 rpm and a (bare electrode) Levich current of 2.49 mA cm^{-2}.

is 3×10^4 M^{-1} s^{-1}, i.e., ca. 10 times larger than the rate constant we measured for the cross-phase electron-exchange reaction. However, it should be recognized that the reaction conditions are quite different in the two sets of experiments. Cross-phase electron exchange is necessarily a surface reaction that proceeds at the interface between the Donnan domains and the surrounding solution, although we chose to express its rate constant in the units of a homogeneous reaction by using conventional three-dimensional concentrations obtained by averaging the actual concentrations over the whole cross section of the film.[19] In this context it would not be surprising if collisions between reactants were less efficient within the polymer film than in homogeneous solution. Indeed, such potential differences in the relative accessibility of attached reactant centers was invoked in an earlier study[4] to account for the much lower reaction rate of Fe^{2+} and $IrCl_6^{3-}$ (by a factor of 10^4) inside coatings of protonated poly(4-vinylpyridine) than in homogeneous solution.[12] The smaller decrease in reaction rate in the present case is likely the result of the much more open structure of the PLL coatings so that the reactant within the Donnan domains remains more accessible for reaction with the coreactant in the solution phase. Of course, large effects on the magnitude of rate constants measured for both self-exchange and cross reactions will result whenever the diffusion-controlled rate within a coating becomes so small that the reactions are no longer activation controlled.[23]

Relative Contributions of i_E and i_S to i_F. It is interesting to consider how the thickness of the coating affects the relative contributions to the total film current of the reactant that is inside and outside the Donnan domains. The vertical distance between the two dashed lines in Figure 6 shows that i_E is more than an order of magnitude larger than i_S. With the thickest films, where the measured values of i_F fall on the asymptote corresponding to $i_E + i_S$, it follows that the reactant within the Donnan domains carries most of the current. With thinner coatings, the larger measured currents become less than the sum of i_S and i_E because the rate of exchange between reactants in the two phases is no longer adequate to maintain full equilibria between them. i_E represents a smaller fraction of i_F under these conditions which corresponds to the sigmoidal portion of the solid curves in Figure 6. With the thinnest films there is no significant contribution to the measured currents from the reactant within the Donnan domains because the $Fe^{III}(edta)^-$ can diffuse through the coating before it has time to exchange electrons or places with $Fe^{II}(edta)^{2-}$ present in the Donnan domains.

(22) Wilkins, R. G.; Yellin, R. E. *Inorg. Chem.* **1968**, 7, 2667.

(23) Buttry, D.; Anson, F. C. *J. Am. Chem. Soc.* **1982**, *104*, 4824.

Reactant Concentration Profiles. It may be helpful in visualizing the processes occurring inside the coating to display how the concentration of $Fe^{III}(edta)^-$ inside and outside the Donnan domains varies across the coating during current flow. Dimensionless concentration profiles inside several of the films listed in Table I were calculated for a fixed electrode rotation rate from eq 27 and 28 of ref 3, and the results are presented in Figure 8. For the thinnest films the concentration of $Fe^{III}(edta)^-$ inside the Donnan domains is zero everywhere in the film (and the concentration of $Fe^{II}(edta)^{2-}$ attains its constant maximum value). Outside the Donnan domains the concentration profile of $Fe^{III}(edta)^-$ is linear and corresponds to the diffusion of the complex through an inert film. The entire film current is provided by i_S. As the film thickness increases, allowing more time for cross-phase electron and place exchange, finite concentrations of $Fe^{II}(edta)^-$ appear within the Donnan domains at steady state, and the two concentration profiles are nonlinear in the portions of the film where the exchange reactions have not reached equilibrium. Finally, with the thickest film, exchange equilibrium is established throughout the film and the two concentration profiles are linear and superimposed everywhere in the film. The film current is now the sum of i_S and i_E. (In terms of the classifications of ref 3, we pass from "R" through "R + S + E" to "S + E" as the thickness of the film is increased.)

Properties of Equation 9. It is important to note that the fitting of rotating disk limiting current data to eq 9 does not require a knowledge of the thickness of the polymer coating. This is a distinct advantage because the thickness of coatings is often one of the least reliably known parameters for polymer-coated electrodes. However, the coating thickness is required to evaluate diffusion coefficients from the experimental values of i_S and i_E (vide supra).

It is clear from the form of eq 9 that film currents measured at polymer-coated rotating disk electrodes will be affected by the kinetics of the self-exchange reaction only within certain ranges of the parameter $(i_k/i_S + i_k/i_E)$. When the second term inside the brackets of eq 9 approaches one of its limiting values of i_S/i_E or zero, the experimental values of i_F are not significantly affected by the kinetics of the self-exchange process and only information about i_E or i_S can be extracted from the rotating disk current measurements. This is the situation corresponding to the two dashed lines in Figure 6. The horizontal separation between these two lines defines the range of coating thicknesses and film currents where the measured currents are affected by the kinetics of the self-exchange reaction. Thus, the best coatings to employ in experiments designed to measure self-exchange rates are those that provide small values of i_S and large values of i_E, i.e., small values of D_S and large values of D_E. It should be noted that there are no circumstances where a direct one-to-one correspondence exists between i_F and i_k. Thus, the simpler procedure employed heretofore[1] to obtain self-exchange rates from limiting currents recorded at coated, rotating disk electrodes requires modification in the light of eq 9. The data analysis procedure described here should be employed in any future studies of self-exchange reactions. However, it should be also recognized that eq 9 will not be obeyed by redox couples with formal potentials that are altered significantly by their incorporation into polyelectrolyte coatings. In such cases the relationships derived for reversible cross-reactions[6] should be employed.

Concentration Dependence of D_S. The values of i_S listed in Table II allow the dependence of D_S on C_A^0, the bulk concentration of the reactant $([Co(C_2O_4)_2(NH_3)_2]^-$, serving as a surrogate for $Fe^{III}(edta)^-$), to be discerned. Figure 9 displays this dependence along with the decrease in the coating thickness that result from increasing C_A^0. The parallel decreases in D_S and Φ are most likely the result of increased cross-linking of the polyelectrolyte chains as more and more $Zn(edta)^{2-}$ (serving as a surrogate for $Fe^{II}(edta)^{2-}$) is incorporated by the Donnan domains. However, the effects are rather modest and the highly open structure of the coatings appears to be preserved as C_A^0 increases.

Would a One-Phase Model for the Coating Be Compatible with the Experimental Data? The good agreement between the calculated and experimental data points in Figure 6 shows that the experimental results can be well accounted for with the two-phase model that led to eq 9. However, it is reasonable to ask whether a single-phase model of the polyelectrolyte coating in which no distinction is made between "Donnan domains" and the solution that surrounds them might also be able to accommodate the experimental results. In such a one-phase model charge transport across the coating would involve a single diffusion process comprised, in general, of both ionic motion and electron hopping between pairs of oxidized and reduced reactants. This composite diffusional process would give rise to a characteristic current density, i_M (similar to i_E) that measured the net rate of charge propagation across the single-phase film. The only place where cross-phase electron- or place-exchange reactions could occur would be at the interface between the coating and the bulk solution. The corresponding characteristic current density for the exchange would be

$$i_{k,M} = F(k_M C_A^0 + k_{2,M})\Gamma_{p,M}^0 \qquad (10)$$

where $\Gamma_{p,M}^0$ represents the surface concentration of a monolayer of the incorporated reactant and k_M and $k_{2,M}$ are rate constants for the self-exchange and interchange reactions analogous to reactions 4, 5, and 7 when they are restricted to the coating–solution interface. The film current density, i_F, would then obey the equation

$$\frac{1}{i_F} = \frac{1}{i_M} + \frac{1}{i_{k,M}} \qquad (11)$$

with $i_{k,M}$ independent of film thickness. The variation of i_F with film thickness will arise only from the dependence of i_M on Φ so that plots of i_F vs. Φ should have the shape shown in Figure 10. The film current can never exceed $i_{k,M}$ no matter how thin the film because the one-phase model provides no pathway for charge transport that does not involve cross-phase exchange at the film–solution interface. The experimental film currents shown in Figure 6 clearly do not fit the curve in Figure 10 which eliminates the possibility of the one-phase model and reinforces the support of the two-phase model.

Charge Transport within the Donnan Domains. Short-time chronocoulometric[24,25] and chronoamperometric[26] measurements

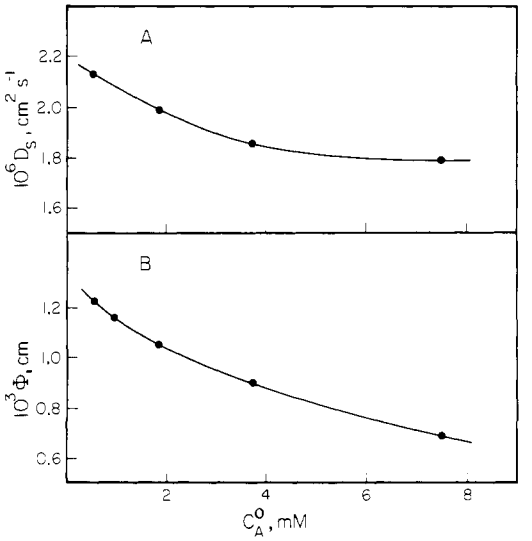

Figure 9. Variation with the bulk reactant concentration of the coating thickness, Φ, and of the reactant diffusion coefficient, D_S, in the solution phase within the PLL coatings. The data were obtained in solutions of $[Co(C_2O_4)_2(NH_3)_2]^-$ and $Zn(edta)^{2-}$ which served as surrogate reactants for $Fe^{III}(edta)^-$ and $Fe^{II}(edta)^{2-}$, respectively (see text).

(24) Oyama, N.; Anson, F. C. *J. Electrochem. Soc.* **1980**, *127*, 640–647.
(25) Oyama, N.; Yamaguchi, S.; Nishiki, Y.; Tokuda, K.; Matsuda, H.; Anson, F. C. *J. Electroanal. Chem.*, in press.
(26) Daum, P.; Lenhard, J. R.; Rolison, D.; Murray, R. W. *J. Am. Chem. Soc.* **1980**, *102*, 4649.

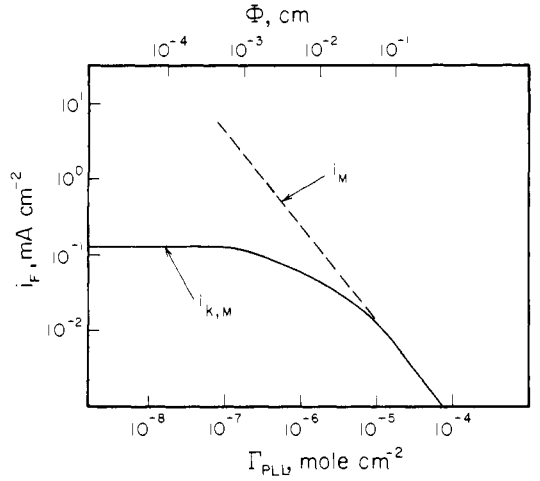

Figure 10. Calculated film currents as a function of coating thickness for a film consisting of a single phase.

with polyelectrolyte-coated electrodes have become common for the estimation of apparent diffusion coefficients for reactants incorporated in the coatings.[25-34] It is of interest to consider the results to be expected from such measurements in light of the model for the coating interior depicted in Figure 1. In cases where polyelectrolyte coatings retain electrostatically bound reactants upon transfer to a pure supporting electrolyte solution, the chronocoulometric or chronoamperometric responses can be related directly to i_E. For example, the slopes of chronocoulometric plots of charge vs. (time)$^{1/2}$, recorded at times short enough so that the diffusion layer within the film is small compared with the film thickness, are related to i_E and D_E as expressed in the equation

$$i_E = \frac{FD_E\Gamma^0}{\Phi^2} = \frac{\pi S^2}{4F\Gamma^0} \tag{12}$$

where Γ^0 is the quantity of reactant remaining in the Donnan domains after the electrode is transferred to the pure supporting electrolyte and S is the chronocoulometric slope. (Note that eq 12 allows i_E to be determined from the chronocoulometric slope without knowing the thickness of the coating.) In writing eq 12 it is assumed that all of the reactant that is not electrostatically held within the Donnan domains is rapidly lost upon transfer to the pure supporting electrolyte solution. Experimental confirmation of this assumption has been obtained with PLL coatings.[34] Some reactants, including $Fe^{II}(edta)^{2-}$ and $Fe^{III}(edta)^-$, depart from the Donnan domains too rapidly in pure supporting electrolyte solutions to allow the straightforward application of eq 12. In such cases it is preferable to carry out the transient chronocoulometric measurements in the presence of the incorporating reactant, but the resulting chronocoulometric slopes then contain contributions from the reactant present outside as well as inside the Donnan domains and the contribution of the former must be subtracted before i_E and D_E can be determined. The slopes may also be affected by coupling between the two types of reactant via the cross-phase electron- and place-exchange reactions. However, the effect of these coupling reactions can be eliminated by employing experimental measurement times too short for the reactions to proceed.

Table IV. Diffusion Coefficient for Charge Transport by $Fe^{II}(edta)^{2-}$ within the Donnan Domains in PLL Coatings[a]

$10^7\Gamma_{PLL}$,[b] mol cm^{-2}	$10^3\Phi$,[c] cm	$10^{10}\Gamma_{Fe(II)}$,[d] mol cm^{-2}	10^4S,[e] C cm^{-2} s$^{-1/2}$	10^6D_E,[f] cm^2 s^{-1}
0.96	0.61	12.6	7.0	7.4
1.28	0.82	16.8	5.5	4.3
1.93	1.23	24.9	6.8	7.2
2.57	1.64	33.3	7.1	7.9
3.85	2.45	49.5	7.0	7.8
5.13	3.27	65.7	7.6	9.45
7.70	4.90	98.6	6.5	6.6
10.3	6.56	129	7.2	8.6
17.8	8.15	161	6.8	7.6
27.9	17.8	385	7.2	7.2
55.8	35.5	731	6.9	7.2
112	71.3	1540	7.0	6.8
224	143	3101	7.3	7.4
				av 7.3

[a] The test solution contained 0.55 mM $Fe^{III}(edta)^-$ and 0.2 M CH_3COONa at pH 5.5. [b] Quantity of PLL in the coatings. [c] Measured micrometrically as described in the Experimental Section. [d] Total quantity of $Fe^{II}(edta)^{2-}$ present in the Donnan domains. [e] Slope of the linear chronocoulometric charge-(time)$^{1/2}$ plot during the first 5 msec after the potential step was applied. [f] Calculated from equation 16 using $D_S = 2.1 \times 10^{-6}$ cm^2 s^{-1}.

The measured chronocoulometric slope, S, will represent the sum of the contributions from the reactant inside and outside the Donnan domains:

$$S_{in} = \frac{2F\Gamma^0}{\Phi}\left(\frac{D_E}{\pi}\right)^{1/2} \tag{13}$$

$$S_{out} = 2F\kappa C_A{}^0\left(\frac{D_S}{\pi}\right)^{1/2} \tag{14}$$

$$S = S_{in} + S_{out} \tag{15}$$

Combining and rearranging eq 13–15 leads to the following expression for D_E:

$$D_E{}^{1/2} = \frac{\Phi}{\Gamma^0}\left(\frac{\pi^{1/2}S}{2F} - \kappa C_A{}^0 D_S{}^{1/2}\right) \tag{16}$$

Equation 16 was used to evaluate D_E from the measured chronocoulometric slopes and film thicknesses. The correction term on the right-hand side of eq 16 was evaluated by using the previously measured values of D_S (Table II, Figure 8).

Two series of chronocoulometric experiments were conducted with measurement times restricted to values (<5 ms) that assured the absence of significant contributions from any cross-phase exchange reactions. For example, at the highest reactant concentration employed ($C_A{}^0$ = 7.5 mM) k_{ap} was only 15 s^{-1}. The first series of experiments was designed to compare the values of D_E resulting from the transient chronocoulometric measurements with those obtained previously from the steady-state rotating disk results. The values of D_E resulting from transient experiments with a fixed concentration of reactant and varying thicknesses of the PLL coating are listed in Table IV. (The most extensive data were acquired for the oxidation of $Fe^{II}(edta)^{2-}$ rather than the reduction of $Fe^{III}(edta)^-$ and these are the data in Table IV. Tests showed that D_E for $Fe^{II}(edta)^{2-}$ and $Fe^{III}(edta)^-$ were essentially equal.) The values of D_E in Table IV are approximately independent of the film thickness, as expected, and the average value, 7.3×10^{-6} cm^2 s^{-1}, is in reasonable agreement with the value obtained from the rotating disk measurements, 6.7×10^{-6} cm^2 s^{-1}.

Concentration Dependence of D_E: Ion Displacement vs. Electron Hopping. In a second set of chronocoulometric experiments the amount of PLL in the coating was fixed and the reactant concentration was varied. The purpose was to determine the de-

(27) Rubinstein, I.; Bard, A. J. *J. Am. Chem. Soc.* **1980**, *102*, 6641; **1981**, *103*, 5007.
(28) Buttry, D. A.; Anson, F. C. *J. Electroanal. Chem.* **1981**, *130*, 333–338.
(29) Facci, J.; Murray, R. W. *J. Electroanal. Chem.* **1981**, *124*, 139; *J. Phys. Chem.* **1981**, *85*, 2870.
(30) Kao, K.-N.; Murray, R. W. *J. Electroanal. Chem.* **1982**, *131*, 37.
(31) Mortimer, R.; Anson, F. C. *J. Electroanal. Chem.* **1982**, *138*, 325.
(32) White, H. S.; Leddy, J.; Bard, A. J. *J. Am. Chem. Soc.* **1982**, *104*, 4811.
(33) Martin, C. R.; Rubinstein, I.; Bard, A. J., *J. Am. Chem. Soc.* **1982**, *104*, 4817.
(34) Anson, F. C., Ohsaka, T., Saveant, J. M. *J. Phys. Chem.* **1983**, 87, 640–647.

Table V. Concentration Dependence of the Diffusion Coefficient for Charge Transport by $Fe^{II}(edta)^{2-}$ within the Donnan Domains

$[Fe^{II}(edta)^{2-}]$,[a] mM	$10^3\Phi$,[b] cm	$10^9\Gamma_{Fe(II)}$,[c] mol cm^{-2}	10^6D_S,[d] cm^2 s^{-1}	10^4S,[e] C cm^{-2} s$^{-1/2}$	10^6D_E,[f] cm^2 s^{-1}
0.55	1.23	2.43	2.13	6.8	7.2
0.94	1.16	4.31	1.93	13.1	9.1
1.87	1.05	8.52	1.99	28.6	7.4
3.74	0.90	17.0	1.86	63.1	7.8
7.48	0.69	33.9	1.79	142	6.0

[a] Supporting electrolyte: 0.2 M CH_3COONa at pH 5.5. [b] Electrodes were coated with 1.9×10^{-7} mol cm^{-2} of PLL. Φ was calculated as described in Table II. [c] Total quantity of $Fe^{II}(edta)^{2-}$ present in the Donnan domains. [d] Diffusion coefficient of the reactant in the solution phase within the coating as measured from rotating disk electrode measurements in solutions of surrogate reactants (see text). [e] Slope of the linear chronocoulometric charge-(time)$^{1/2}$ plot during the first 5 msec after the potential step was applied. [f] Calculated from eq 16.

pendence (if any) of D_E on the concentration of reactant inside the Donnan domains in order to assess the relative importance of ionic motion and electron hopping to the propagation of charge within the Donnan domains. The results, summarized in Table V, show that D_E exhibits no systematic sensitivity to the reactant concentration over the concentration range investigated. This concentration independence of D_E points to ion displacement instead of electron hopping as the predominant charge-transport process within the Donnan domains.[24,27] D_E can be divided into two components:

$$D_E = D_E^i + D_E^e \quad (17)$$

where D_E^i is the diffusion coefficient corresponding to ion displacement and D_E^e is the diffusion coefficient corresponding to electron hopping. The latter can be estimated as[18]

$$D_E^e = C_p^* k_{ex} d_e^2 \quad (18)$$

where C_p^* is the concentration of the electroactive reactant in the Donnan domains, k_{ex} is the rate constant for the electron exchange between reactant pairs, and d_e is the distance between the reactants when the electron hops. This relationship seems more suited for electron-exchange contributions to single-file diffusion[18] than the similar relationships derived by Dahms[17] and Ruff et al.[35] for three-dimensional diffusion in solution although both approaches lead to very similar results. The concentration, C_p^*, called for in eq 18, is the actual microscopic concentration of reactant ($Fe^{II}(edta)^{2-}$) within the Donnan domains instead of its average value through the coating, Γ_p^0/Φ. The dry density of PLL (2.35 g cm^{-3} for the hydrobromide salt[14]) corresponds to a concentration of NH_3^+ sites of ca. 11 M. The largest value of $\Gamma_{Fe(II)}$ in Table V corresponds to ca. 0.18 mol of $Fe^{II}(edta)^{2-}$ per mole of NH_3^+ sites corresponding to a local concentration of $Fe^{II}(edta)^{2-}$ within the Donnan domains of ca. 2 M. The value of d_e should be approximately equal to the separation between reactant centers when they are in close contact, ~10 Å, so that k_{ex} would have to be rather large for D_E^e to make a significant contribution to D_E. For example, even if D_E^i were as small as 10^{-8} cm^2 s^{-1}, k_{ex} would have to exceed 5×10^6 M^{-1} s^{-1} for D_E^e/D_E^i to be larger than 0.1. The estimated value of k_{ex} for the $Fe^{III/II}(edta)$ couple in homogeneous solution is only 3×10^4 M^{-1} s^{-1},[22] and it is not likely to exceed this value significantly for ions confined to the Donnan domains. Therefore electron hopping between $Fe^{II}(edta)^{2-}$ and $Fe^{III}(edta)^-$ would not appear to be a significant component of the mechanism of charge transport within the Donnan domains. Recall, however, that we have previously identified the cross-phase electron-exchange reaction between these two reactants as the primary mechanism for coupling between the charge-transport processes that proceed inside and outside the Donnan domains. Indeed, the presence of the central, nonlinear portions of the solid curves in Figure 6 depends upon the occurrence of cross-phase coupling reactions. Thus, we conclude that electron transfer between pairs of oxidized and reduced reactants in separate phases that proceeds rapidly enough to produce significant coupling between the rates of reactant diffusion in both phases may, nevertheless, proceed too slowly when both reactants are in the same phase to affect the net rate of reactant diffusion in that phase. Of course, this result depends very strongly on the magnitude of D_E^i. With polyelectrolyte coatings that produce much smaller values of D_E^i, electron self-exchange processes could contribute importantly to both cross-phase coupling and in-phase facilitation of charge transport.

Relative Magnitude of D_S and D_E. The value of D_S obtained from the measurements with the rotating disk electrode, 2×10^{-6} cm^2 s^{-1}, is somewhat smaller than the diffusion coefficient of $Fe^{III}(edta)^-$ in solution as estimated from the slope of the dashed line in Figure 5; $D = 4 \times 10^{-6}$ cm^2 s^{-1}. By contrast, the measured value of D_E, 6.7×10^{-6} cm^2 s^{-1}, is larger than the solution diffusion coefficient despite the apparent absence of any electron-exchange contribution to the diffusion. This is a surprising result since it indicates that diffusional motion of the complex that is held electrostatically within the Donnan domains may be more rapid that its unencumbered diffusion in homogeneous solution as well as in the solution phase within the PLL coating. It should be recognized that in the evaluation of D_E the square of the coating thickness enters the calculation so that errors in estimating the thicknesses of the swollen PLL coatings lead to larger errors in the values of D_E. However, the coating thickness would have had to be ca. 70% of the measured values to account for the difference between D and D_E, and we do not believe the errors in measurement were that large.

The relatively large values of D_E^i that we observe may be an indication that ion hopping rather than solution-like diffusion is the mechanism of ionic displacement within the Donnan domains. Ion–ion interactions of the Fuoss–Onsager type[36] within the Donnan domains would be expected to decrease solution-like diffusion rates to values smaller than those in the surrounding solution within the film or in the bulk solution. Ion pairing within the Donnan domains could produce even larger decreases in diffusion rates. On the other hand, ion hopping between neighboring sites could occur in an environment containing a lower density of retarding water molecules because of the intrinsic hydrophobicity of the polymer chain backbone and the high ionic strength in the Donnan domains. The open structure of PLL films, consistent with their extensive swelling, should result in relatively little cross-linking, leaving the polymer chains flexible enough to pass through conformations that provide close contacts between the charged sites on the same and other chains. Such diffusion by ion hopping could be the main reason that the diffusion of $Fe^{III}(edta)^-$–$Fe^{II}(edta)^{2-}$ anions (as well as other incorporated anions[34]) proceeds so rapidly in PLL films. It is also in accord with the much slower diffusional rates observed in other types of polymer films, such as Nafion,[23,27,28,32,33] because these polymers are more rigid and less swollen and would be expected to require higher free energies to place neighboring ionic sites in close contact.

Concluding Remarks

The primary purpose of this study was to demonstrate the viability of the two-phase model for the interior of polyelectrolyte films depicted in Figure 1. Some of the consequences of this model, such as the two modes of charge transport within the film and the importance of coupling between them, have been established for the case of $Fe^{III}(edta)^-$–$Fe^{II}(edta)^2$ in PLL coatings. The coupling is accomplished by electron-exchange and/or place-exchange reactions between two reactants in different phases. The coupling serves to increase the overall charge transport rate by accentuating the role of the more rapid of the two transport

(35) Ruff, I. *Electrochim. Acta* **1970**, *15*, 1059. Ruff, I.; Korosoi-Odor, I. *Inorg. Chem.* **1970**, *9*, 186. Ruff, I.; Friedrich, V. J. *J. Phys. Chem.* **1971**, *75*, 3297. Ruff, I.; Friedrich, V. J.; Demeter, K.; Csillag, K. *Ibid.* **1971**, *75*, 3303.

(36) Fuoss, R. M.; Onsager, L. *J. Phys. Chem.* **1962**, *66*, 1722; **1963**, *67*, 621; **1964**, *68*, 1.

modes. Structural differences among polyelectrolyte coatings are anticipated to produce quantitative variations in the relative importance of the two phases in charge propagation and in the importance of coupling between the propagation pathways in each phase. The rates of all three processes appear to be remarkably high with PLL coatings in which $Fe^{III/II}$(edta) anions are incorporated. The highly swollen, flexible structure provided by the PLL coatings appears to be the common basis for the high rate of all three processes.

The use of variations (if any) in reactant diffusion coefficients to distinguish between ion hopping and electron hopping as the mechanism of charge transport within the Donnan domains was also demonstrated. The form of the general equation for the steady-state electrochemical behavior of redox self-exchange reactions at polyelectrolyte-coated electrodes (eq 9) requires revision in the previously suggested[1] formula for estimating electron-exchange rate constants.

Although the two-phase model of Figure 1 has been tested for the case of $Fe^{III/II}$(edta) in PLL, we believe the essential features of the model and the consequences to which they lead should be generally applicable to polyelectrolyte-coated electrodes.

Acknowledgment. This work was supported in the U.S.A. by the National Science Foundation and the U.S. Army Research Office and in France by the CNRS (Equipe de Recherche Associeé 309 "Electrochimie Moleculaire", ATP, "Epargnes d'Energie et de Matieres Premieres"). We are grateful to Claude P. Andrieux, Daniel Buttry, and Takeo Ohsaka for numerous helpful discussions and to the North Atlantic Treaty Organization for a Collaborative Research Grant.

Registry No. Fe^{II}(edta)$^-$, 15275-07-7; Fe^{III}(edta)$^{2-}$, 15651-72-6; Fe^{III}(Heedta), 17084-02-5; $[Co(C_2O_4)_2(NH_3)_2]^-$, 39141-87-2; Zr^{II}(edta)$^{2-}$, 12519-36-7; CH_3COONa, 127-09-3; PLL, 26588-20-5; graphite, 7782-42-5.

Transient Spontaneous Raman Study of Photoionization Kinetics at the Hydrocarbon/Water Interface in Micellar Solutions

S. M. Beck and L. E. Brus*

Contribution from Bell Laboratories, Murray Hill, New Jersey 07974. *Received June 8, 1982*

Abstract: Transient spontaneous Raman spectroscopy (416 nm) has been used to observe the kinetics of TMB^+ and TMB^{2+} ions following photoionization of tetramethylbenzidine (TMB) in aqueous micellar solutions. The ground-state TMB pK_a values are shifted by micellar solubilization in the directions predicted by calculated surface pH values. In SDS micelles, the TMB^+ ion initially produced is stabilized by negative surface groups. No time evolution of the TMB^+ Raman spectrum occurs, and bimolecular ion reactions are not observed. However, in CTAB micelles, TMB^+ is destabilized by positive surface groups. The TMB^+ Raman spectrum evolves on the 10^{-6}-s time scale, suggesting that the ion has moved into the Stern layer and is asymmetrically solvated. On the 10^{-4}-s time scale, TMB^{2+} appears from disproportionation of two TMB^+ ions. Positive spectral identifications are facilitated by comparison with spectra obtained by chemical oxidation in various environments.

Introduction

Condensed-phase chemical reactions are often strongly dependent upon solvation. In enzymes and membranes, a coordinated local arrangement of solvating molecules can completely control a reaction in the catalytic sense. These systems are often microscopically heterogeneous, in that a region of hydrophobic character exists within a few ångströms of a region of hydrophilic character. Aqueous micellar solutions provide a simple example exhibiting similar structural features. A hydrocarbon-like micellar interior, of perhaps 40-Å diameter, is separated from an aqueous phase by an ionic double-layer boundary region. A static potential gradient exists across the boundary region. This gradient is of opposite sign in cationic and anionic micelles. Recent experiments have utilized such systems to permanently separate charge following photoionization, and to preferentially stabilize organic cations in the interior of anionic micelles.[1]

A given molecular species can be preferentially stabilized in the interior of a micelle, on its boundary (Stern layer), or in the aqueous phase, depending upon the balance of hydrophobic and hydrophilic interactions and the sign of the surface potential. Aromatic neutral molecules often dissolve in the hydrocarbon-like micelle interior. A pulse of light can photoionize such species, with the ejected electron becoming solvated in the aqueous phase. The resulting molecular anion might be preferentially stabilized in the boundary region or the aqueous phase. In some systems, then, an initial photoionizing pulse may create a cation which subsequently moves out from the micelle interior. The ejected electron could be captured by a preexisting different cation in the boundary double layer region, with the result that the reduced species moves in toward the micellar interior. Thus, in time-resolved, pump–probe spectroscopic experiments, one might monitor the motion of transient species across the double-layer region.

Transient electronic absorption offers excellent detection sensitivity, yet provides little structural information because of the diffuse nature of the spectra. Transient spontaneous Raman spectroscopy, yielding direct vibrational information, offers a number of advantages in the study of chemical kinetics. This application has been clearly demonstrated in previous examples of homogeneous solution reactions.[2] In this paper we apply Raman spectroscopy to the study of molecular motion and reaction in micellar solutions. We have previously noted the feasibility of hydrocarbon/aqueous interface kinetics studies, and the enhanced detection sensitivity of transient Raman experiments, in micellar solutions.[3] The essential question is the degree to which the spectra are sensitive to the nature of the local environment. A similar question has been addressed in hemoglobin studies,

(1) (a) N. J. Turro, M. Grätzel, and A. M. Braun, *Angew. Chem., Int. Ed. Engl.*, **19**, 675 (1980); (b) J. K. Thomas, *Acc. Chem. Res.*, **10**, 133 (1977).

(2) (a) S. M. Beck and L. E. Brus, *J. Chem. Phys.*, **75**, 4934 (1981); (b) R. F. Dollinger and W. F. Woodruff, *J. Am. Chem. Soc.*, **101**, 4391 (1979); (c) R. Wilbrant, P. Paqsberg, K. B. Handson, and K. V. Weisberg, *Chem. Phys. Lett.*, **36**, 76 (1975).

(3) S. M. Beck and L. E. Brus, *J. Chem. Phys.*, **75**, 1031 (1981).

0002-7863/83/1505-1106$01.50/0